Surface Chemistry

International Edition: DOI: 10.1002/anie.201915024
German Edition: DOI: 10.1002/ange.201915024

Real-Time Atomic-Scale Visualization of Reversible Copper Surface Activation during the CO Oxidation Reaction

Langli Luo[+], Yao Nian[+], Shuangbao Wang[+], Zejian Dong, Yang He, You Han,* and Chongmin Wang**

Abstract: *By using in situ aberration-corrected environmental transmission electron microscopy, for the first time at atomic level, the dynamic evolution of the Cu surface is captured during CO oxidation. Under reaction conditions, the Cu surface is activated, typically involving 2–3 atomic layers with the formation of a reversible metastable phase that only exists during catalytic reactions. The distinctive role of CO and O_2 in the surface activation is revealed, which features CO exposure to lead to surface roughening and consequently formation of low-coordinated Cu atoms, while O_2 exposure induces a quasi-crystalline CuOx phase. Supported by DFT calculations, it is shown that crystalline CuOx reversibly transforms into the amorphous phase, acting as an active species to facilitate the interaction of gas reactants and catalyzing CO oxidation.*

Introduction

The interaction between gas molecules and catalyst surface is of fundamental importance in heterogeneous catalysis. It has been generally realized that catalysts experience both structural and chemical changes, as directly revealed by emerging in situ characterization methods,[1] which is critical to catalytic processes under reaction conditions. For noble metal catalysts such as Pt and Au, the adsorbed CO molecules can cause the metal surface atoms to restructure[2] and morphological change of supported nanoparticles has also been reported.[3] For transition-metal catalysts such as Cu, the structural and chemical change of the active species should be more vigorous because of the tendency of the valence change of metals. For instance, the Cu/ZnO catalyst for methanol synthesis has been readily reported to experience redox reaction[4] and strong interaction between ZnO support and Cu involving both structural and chemical changes.[5] For Cu as electrocatalysts, surface states of oxide-derived Cu plays a critical role in the electrochemical conversion of CO to liquid fuels but remains largely unknown.[6] Understanding surface behaviors of the transition metal catalysts especially obtaining in situ dynamic information under reaction conditions are essential to identify active sites that lead to the deciphering of the reaction mechanisms.

Specifically, the atomistic process of surface and subsurface dynamics for Cu catalysts in redox reaction remains largely unclear. Exemplified by the water gas shift (WGS) reaction and CO oxidation reaction involving either oxidizing (O_2 or H_2O) and reducing gases (CO), the valence variation of Cu plays a significant role in catalyzing the reactions. Cu_2O phase has been proposed to be more active than pure Cu and CuO based on the studies of nanoparticle catalysts with three phases[7] and Cu_2O nanocrystals have been reported to undergo in situ surface oxidation during the reaction.[8] Surface oxides exist on Cu catalysts exposed to air and even after pretreatment/annealing under an O_2-rich reaction condition (1 at% CO in air is usually used in performance test) in accordance with in situ spectroscopy results.[9] Structurally, the reactant gases could re-arrange surface atoms of Cu that the Cu(111) surface with compact and the lowest energy surface, can be activated by CO adsorption to form mobile clusters and become activated for water dissociation in WGS reaction.[10] These observations highlight the strong interaction between Cu and CO deviated from canonical scenario that needs further investigation. Herein, we use AC-ETEM to visualize atomic-scale dynamics on pure Cu surface under CO oxidation reaction conditions ($CO + O_2$ gas mixture and elevated temperature), where the Cu surface is activated through atomic rearrangement down to 2–3 atomic layers. We also discovered distinctive structural responses to the exposure of CO and O_2 on the Cu surface, and the unique role of surface CuO_x species formed on the Cu surface is identified under the real gas reaction conditions. Density functional theory (DFT) calculation and ab initio molecular dynamics (AIMD) simulation corroborate the experimental observa-

[*] Prof. Dr. L. Luo,[+] Z. Dong
Institute of Molecular Plus, Tianjin Key Laboratory of Molecular Optoelectronic Sciences, Department of Chemistry
Tianjin University
92 Weijin Road, Tianjin 300072 (China)
E-mail: luolangli@tju.edu.cn

Y. Nian,[+] Prof. Dr. Y. Han
School of Chemical Engineering and Technology, Tianjin University and Collaborative Innovation Center of Chemical Science and Chemical Engineering (Tianjin)
Tianjin 300350 (China)
E-mail: yhan@tju.edu.cn

Dr. S. Wang[+]
School of Physical Science and Technology, Guangxi University
Nanning 530004 (China)

Y. He, Dr. C. M. Wang
Environmental Molecular Sciences Laboratory
Pacific Northwest National Laboratory
902 Battelle Blvd, Richland, WA 99354 (USA)
E-mail: chongmin.wang@pnl.gov

[+] These authors contributed equally to this work.

Supporting information and the ORCID identification number(s) for the author(s) of this article can be found under: https://doi.org/10.1002/anie.201915024.

tion on the nature of CuO_x species and its implications for catalytic reactions.

Results and Discussion

We use single-crystal Cu thin films to create low-index surfaces for atomic-scale imaging and make real-time video recording in AC-ETEM. The detailed experimental setup is described in Methods in the Supporting Information. The in situ observations are made on (100) and/or (110) surfaces of the Cu from a cross-sectional view (Supporting Information, Figure S1). Single CO or O_2 or a gas mixture of CO and O_2 with an atomic ratio $CO/O_2 \approx 2{:}1$ at about 1×10^{-4} mbar is introduced to the Cu surface at 350 °C inside the microscope column. It should be noted that we choose the stoichiometric ratio rather than CO 1 %-Air for the CO oxidation reaction as we focus on the atomistic mechanisms under a thermodynamic equilibrium status while not introducing any kinetic effects.

Cu Surface Activation under Reaction Conditions

Real-time atomic-scale structural change on a Cu(100) surface after gas mixture introduction was captured by time-resolved high-resolution (HR)TEM images (Figure 1). First, a clean Cu(100) surface under vacuum (ca. 1×10^{-8} mbar) is shown in Figure 1 a. After 201 s of exposure to the gas mixture, Cu surface atoms slightly deviate from their original positions both laterally and vertically as shown in Figure 1 b. This is induced by the adsorption of CO and O_2 gas molecules, and it continues to evolve into the subsurface with increasing exposure time, leading to the atomic rearrangement of the first two atomic layers (ca. 3.6 Å) of Cu(100) surface as shown in Figure 1 c. A clear interface (red dashed line) separates the activated surface atoms of disordered phase from perfect bulk Cu face-centered cubic (FCC) lattice, and this surface region finally reaches a thickness of about 4.4 Å after 824 s gas exposure (Figure 1 d). The whole activation process is also illustrated by the representations in Figure 1 a–d, where we hypotheses that the CO molecules drag the surface atoms out of their original position and O atoms generated through O_2 chemisorption penetrate into the subsurface. We will discuss the different roles of two reactant gases in detail later. We evaluate the degree of atomic structure change on the Cu surface during the reaction by comparing the lateral strain induced by atomic rearrangement during the surface activation process. A significant increase of surface strain before and after gas exposure is found as shown in strain analysis results (Figure 1 e,f), respectively. The strain caused by strong gas–metal interaction increases the total free energy of the Cu surface and should be counteracted by the gas adsorption energy and the chemical potential of the CO oxidation reaction. Another noting phenomenon is that once we remove the gas mixture, the surface restores to a perfect FCC structure (Supporting Information, Figure S2), indicating this surface activated structure is, in nature, a metastable phase, that only exists during catalytic reactions.

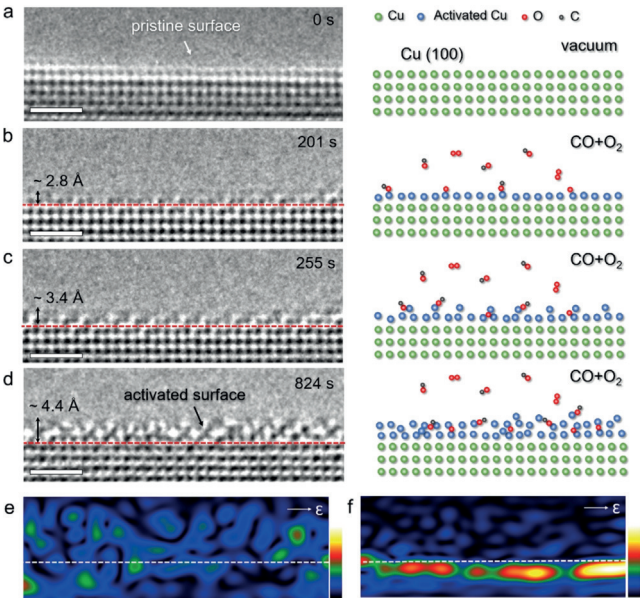

Figure 1. Cu surface atomic re-arrangement under CO oxidation reaction. a)–d) Time-resolved HRTEM image showing a surface activation process of a Cu(001) surface. a) HRTEM image of a pristine Cu(001) surface without any surface restructuring under vacuum (1×10^{-8} mbar) at 350 °C. b) HRTEM image shows the surface layer is activated after 201 s exposure to a $CO + O_2$ gas mixture (atomic ratio CO/O_2 ca. 2:1 at a pressure of ca. 1×10^{-4} mbar at 350 °C). c) HRTEM image showing the first two atomic layers on the Cu(100) surface are activated with a quasi-periodic atomic arrangement. d) HRTEM image shows a surface region (thickness ca. 4.4 Å) with disordered structure is formed on a Cu(100) surface after 824 s. The interface (dashed line) separates activated surface atoms with perfect bulk Cu lattice. e),f) Strain analysis of surface region before and after gas exposure corresponding to HRTEM images in (a) and (d). Scale bars: 1 nm.

To decipher different roles of reactant gases in the activation process, we expose Cu surface to CO and O_2, respectively, under the same gas partial pressure and temperature (350 °C). Similarly, under high vacuum, the Cu surface shows gradually curved atomic steps forming a smooth surface (Figure 2 a). Upon CO exposure (ca. 6.5×10^{-5} mbar), the smooth Cu surface becomes rough and exposes more low-coordinated surface atoms (Figure 2 b). An enlarged HRTEM image (upper, Figure 2 c) shows that surface atoms and some of the subsurface atoms largely re-arranged themselves under CO gas. The atomic positions of these atoms are deviated from the original positions in FCC structure and more steps and kinks are seen on reconstructed Cu(001) surface. This perturbation of atomic arrangement in the surface region is induced by strong CO adsorption and bonding with Cu atoms. This finding is in accordance with recent reports that strong interaction between Cu and CO leads to the formation of protruded surface structure.[10] In distinct contrast, the O_2 exposure leads to lattice expansion near the step edges on a stepped Cu(001) surface (from Figure 2 d to 2e). When introducing O_2 gas at a pressure of about 3.5×10^{-5} mbar, the Cu(002) plane distance increases from 1.81 Å to 2.1 Å (upper, Figure 2 f), and a metastable surface oxide appears near the step-edge (labeled by the white arrow in Figure 2 e). It is noted that the lattice expansion is more prominent near the

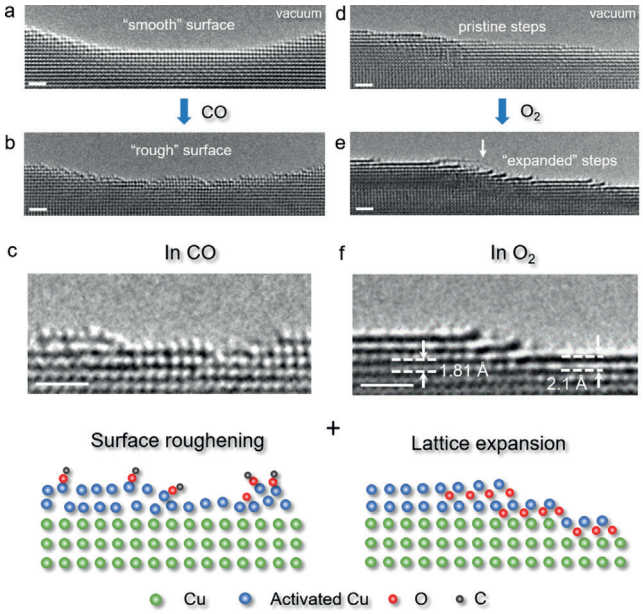

Figure 2. Cu surface atomic rearrangement upon responding to CO and O_2 gases. a) HRTEM image shows a pristine smooth Cu surface under vacuum (1×10^{-8} mbar) at 350 °C. b) HRTEM image shows a reconstructed rough Cu surface under CO (6.5×10^{-5} mbar) at 350 °C. c) Enlarged area from (b) and representation of Cu surface structural change responding to CO. d) HRTEM image shows a pristine stepped Cu(001) surface under vacuum (1×10^{-8} mbar) at 350 °C. e) HRTEM image shows an expanded Cu stepped surface under O_2 (3.5×10^{-5} mbar) at 350 °C. f) Enlarged area from (e) and reporesentation of Cu surface structural change responding to O_2. Scale bars: 1 nm.

step edge, which indicates subsurface diffusion of O through the step edge largely contributes to the lattice expansion. Based on electron energy-loss spectroscopy (EELS) analysis (Supporting Information, Figure S7) on the surface region, we identify both O and Cu edges under this low-pressure O_2 environment, indicating that the surface lattice expansion is induced by O and Cu interaction. These observations are in accordance with our previous Cu surface oxidation studies where step-edges serve as a significant source of nucleation of surface oxides under relatively low gas pressure.[11] The above results reveal that CO and O_2 gases play different roles in activating Cu surface, that is, CO attracts surface Cu atoms by strong Cu–CO bonding and penetrates through the Cu surface by the aid of O_2 which induces top surface lattice expansion.

Role of Surface Oxide in CO Oxidation

Under real CO catalytic reaction conditions, especially the O_2-rich gas environment (1 vol% CO balanced with air), the Cu is covered with surface oxides. As shown in the Supporting Information, Figure S3, once in contact with air, the Cu thin film deposited in UHV evaporation apparatus has been covered with a considerable amount (ca. 5 nm in thickness) of native oxide (Cu_2O). Even at a very low oxygen pressure, the Cu surface can have O_2 chemisorption and surface oxide can be readily formed through a step-edge growth mechanism.[11a] A recent study shows that the metallic Cu phase is only maintained under conditions where close to full oxygen conversion is achieved in the CO oxidation reaction.[9a] We have also found such surface oxides in our gas experiments given that we have removed native oxides by annealing in H_2 gas. The existence of these surface oxides may largely affect the catalytic behaviors of Cu catalysts in terms of altering the gas adsorption and mass/electron transfer. Thus, we further study the structural dynamics of surface oxides on Cu under different gas environments. Figure 3a

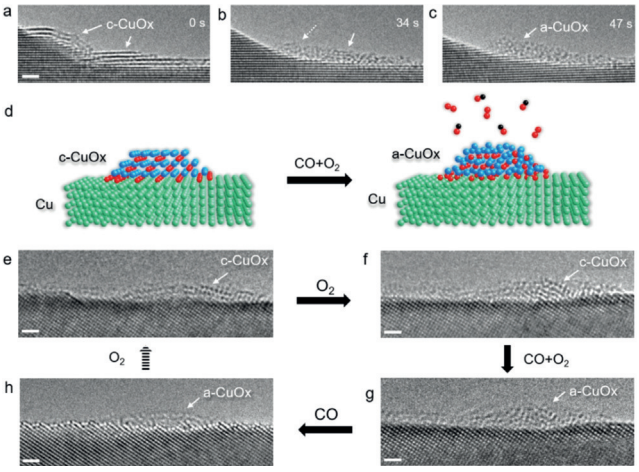

Figure 3. Atomic-scale dynamics of Cu oxide under CO oxidation reactions. a)–c) Time-resolved HRTEM images showing Cu surface oxides are activated under CO oxidation reaction (atomic ratio $CO:O_2=2:1$ at a total pressure of 1×10^{-4} mbar) at 350 °C. d) Representation of crystalline to amorphous transition of surface CuO_x upon CO oxidation reaction. e)–h) Genesis of surface oxide in various gas conditions (Detailed experimental procedures in Supporting information). A two-layer surface oxide c-CuO_x in vacuum (e) grows to 4–5 atomic layers in pure O_2 (f). When the c-CuO_x is exposed to the $CO+O_2$ mixture gas, it changes to amorphous-phase a-CuO_x (g). The c-CuO_x decreases by size in pure CO gas environment (h).

shows a few layers of surface oxide at the step-edge (white arrows) have a crystalline phase (labeled as c-CuO_x) with an expanded lattice space (ca. 2.1 Å) comparing with that of Cu substrate (002) space (ca. 1.8 Å) and is considered as the product of O_2 chemisorption induced surface reconstruction as that shown in Figure 2e. Upon gas mixture ($CO+O_2$) exposure, this c-CuO_x experiences vigorous structural change and transforms into an amorphous phase within a minute as shown in Figures 3b and c. The whole atomic-scale dynamic process is captured by the Supporting Information, Supplementary Video S1, depicting a gradual transition from crystalline to amorphous phase through a layer-by-layer process. As shown in Figure 3b, this phase transition first takes place on the oxide covering step-edge (dashed-line arrow) and after it finishes the phase transition, the oxide on the terrace still possess a crystalline phase to some extent (solid white arrow), which indicates his phase transition is kinetically dependent on local structures (for example, steps). After 47 s, c-CuO_x finishes the crystalline to amorphous phase

transition and being activated. This a-CuO_x keeps a dynamically evolving atomic structure (Supporting Information, Video S1 and Figure S8). This phenomenon is firstly observed here for a surface Cu oxide, as illustrated in Figure 3d.

Moreover, this crystal-to-amorphous phase transition can be reversibly oscillated by alternating between CO and O_2 gas environments. The effect of CO and O_2 to surface oxides can be disentangled in catalytic reaction through in situ observations under a full cycle of various gas conditions (Figure 3e–h, in clockwise order). First, a c-CuO_x island exists on a Cu(110) surface (Figure 3e). Upon O_2 introduction, this c-CuO_x island grows from two atomic layers to 4–5 layers within a few minutes (Figure 3f). Then, we introduce CO gas to achieve a mixture gas with an atomic ratio between CO and O_2 ca. 2:1, the crystalline phase starts to become amorphous and activated (Figure 3g) similar to that shown in Figure 2a–d, which can be seen as the true structure under real reaction conditions. After O_2 gas is removed, the surface oxides are gradually reduced with their dimension decreased (Figure 3h). Finally, we could restore the structure to c-CuO_x by changing gas to pure O_2 gas. These in situ observations not only confirm that the crystalline to amorphous phase transition can happen in the $CO + O_2$ gas mixture but also reveal that the CO destabilize the surface oxides while O_2 builds up the surface oxides.

To explore the origin of these dynamic structural changes of surface oxides on Cu surface under different gas environments, we employed DFT based AIMD simulation to investigate above gas–oxide interactions. First, we start from a classic missing-row reconstructed Cu surface induced by O_2 chemisorption as a stable configuration which is proved by both experiments and calculations.[12] To reflect the configuration of multilayer surface oxide on the Cu surface (Figure 3a), two double-layer missing-row Cu_xO structures on Cu(100) surface was built and misplaced here. Compared with the ordered double-layer missing-row reconstruction, the misplaced double-layer missing-row Cu_xO structure is more stable (Supporting Information, Figure S4) and closer to the polygonal structure in the Cu_xO observed in Figure 3a. Thus, the misplaced double-layer missing-row Cu_xO on the Cu(100) surface was chosen as the Cu_xO/Cu(100) configuration for the following DFT and AIMD calculations.

All of the adsorption sites of reactants and corresponding adsorption energies are shown in the Supporting Information, Figure S5 and Table S1. Compared with other sites, CO prefers perpendicularly adsorbing at site 3 and O_2 prefers to stay at site 4 parallel to CO. The most stable configurations for CO and O_2 adsorption are shown in Figure 4a,b. Although their adsorption energies are almost equal with each other (−1.26 and −1.27 eV, respectively), their favorable adsorption sites are different, indicating that there is no competitive adsorption between CO and O_2. Both the Mulliken charge analysis (Supporting Information, Table S2) and the electron density difference (EDD) analysis (Figure 4a,b) confirm that the electrons transfer from Cu_xO surface to CO and O_2 reactants through Cu–C and Cu–O chemical bonds.

Based on the analysis of CO and O_2 adsorption on the Cu_xO/Cu(100) surface, the mechanism that the structural changes of Cu_xO crystal under CO and O_2 reaction conditions

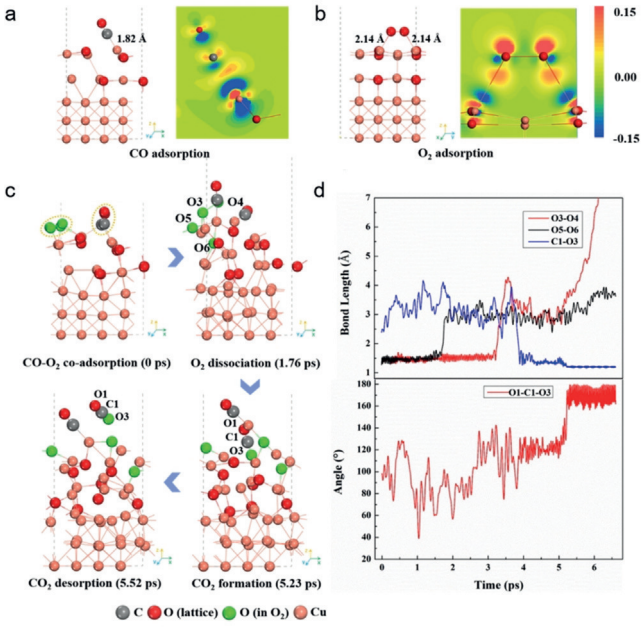

Figure 4. DFT and AIMD calculations for the adsorption of reactants and CO oxidation reaction. a) Stable configuration and EDD patterns of CO adsorption on Cu_xO surface. b) Stable configuration and EDD patterns of O_2 adsorption on Cu_xO surface. c) Structural reconstruction of Cu_xO under CO and O_2 environments via AIMD calculations (NVT, reaction temperature: 350 °C). d) Statistical change of bond lengths and O1-C1-O3 angle during CO oxidation reaction.

observed in the experiments were performed by AIMD simulations. Monolayer coverage with two CO and two O_2 molecules on the Cu_xO/Cu(100) surface is considered as the initial configurations for the AIMD calculations (Figure 4c). After about 1.76 ps evolution, the first O_2 molecules dissociate with two of O atoms bonding to surface Cu atoms. With the help of enough vacancy produced by the upward displacement of surface Cu atom bonding to CO molecule, the dissociated O6 atom migrates and bonds to the subsurface Cu atoms (Supporting Information, Video S2). The dissociation process of the second O_2 molecule occurs at about 3.25 ps and the dissociated O3 atom bonds to surface Cu atoms while dissociated O4 atom migrates and bonds to the subsurface Cu atoms (Supporting Information, Video S3). The length changes of O3–O4 and O5–O6 bonds (Figure 4d) further confirmed the O_2 dissociation. Due to the diffusion of the dissociated O atoms in the Cu_xO structure, the original lattice O atom is forced to migrate to the interface of Cu_xO and Cu(100), resulting in the partial oxidation of Cu metal. These processes lead to the crystal distortion in the Cu_xO/Cu(100) configuration and further result in the amorphization of the Cu_xO crystal as observed in the experiments.

After the dissociation of the adsorbed O_2 molecules, the dissociated O3 atom which bonds to surface Cu atoms gradually migrates to the vicinity of CO and bonds to CO to form CO_2. The change of C1–O3 distance and O1-C1-O3 angle with the simulation time (Figure 4d) further confirmed the formation of CO_2 product. Once the CO_2 molecule is formed, it desorbs easily from the catalyst surface (Supporting Information, Video S4). Therefore, the reaction mechanism

of CO oxidation on the active Cu_xO catalyst is not the same as the Mars-van-Krevelen (MvK)[8,13] mechanism that happened on the Cu_2O surface. For the MvK mechanism, the CO first reacts with the lattice O atom to produce CO_2, which would produce an oxygen vacancy at the Cu_2O surface. Then, the O_2 molecule dissociates at the O vacancy. Whereas on the active Cu_xO surface, the O_2 molecules dissociate firstly into the lattice due to the unsaturated coordination of Cu atoms in the Cu_xO crystal. Then, the adsorbed CO get a lattice O atom to produce CO_2. In general, the strong chemical interaction between CO and Cu at Cu_xO surface could help the dissociation of O_2 molecule and the migration of dissociated O atoms into the Cu_xO lattice, facilitating the CO oxidation reaction while we observed the amorphization process of the c-Cu_xO.

Conclusion

We have observed real-time surface dynamics on Cu at atomic-scale under CO oxidation reaction conditions by AC-ETEM. While pure CO induces surface roughening and O_2 tends to incorporate with surface atoms resulting in surface lattice expansion, the Cu surface can be activated down to two atomic layers upon $CO + O_2$ gas mixture exposure. Under CO oxidation reaction conditions, the universally existing surface oxides can be activated with a dynamic evolving atomic structure, vigorously interacting with CO and O_2 molecules, which reflects the true structure of active species on the Cu surface. We rationalize these observations with the aid of DFT calculation and AIMD simulation, highlighting the role surface oxides in catalytic CO oxidation reaction, which may be extended to other catalytic redox reactions.

Acknowledgements

The authors appreciate the support from the National Natural Science Foundation of China (Grant No. 21873069 and No. 11504162). C.M.W. is supported by the laboratory directed research at Pacific Northwest National Laboratory. Part of the work was conducted in the William R. Wiley Environmental Molecular Sciences Laboratory (EMSL), a DOE User Facility operated by Battelle for the DOE Office of Biological and Environmental Research. Pacific Northwest National Laboratory is operated for the DOE under Contract DE-AC05-76RL01830.

Conflict of interest

The authors declare no conflict of interest.

Keywords: atomic scale · CO oxidation · copper · electron microscopy · environmental TEM

How to cite: *Angew. Chem. Int. Ed.* **2020**, *59*, 2505–2509
Angew. Chem. **2020**, *132*, 2526–2530

[1] a) F. Tao, P. A. Crozier, *Chem. Rev.* **2016**, *116*, 3487–3539; b) M. Duan, J. Yu, J. Meng, B. Zhu, Y. Wang, Y. Gao, *Angew. Chem. Int. Ed.* **2018**, *57*, 6464–6469; *Angew. Chem.* **2018**, *130*, 6574–6579.

[2] a) H. Yoshida, Y. Kuwauchi, J. R. Jinschek, K. Sun, S. Tanaka, M. Kohyama, S. Shimada, M. Haruta, S. Takeda, *Science* **2012**, *335*, 317–319; b) T. Avanesian, S. Dai, M. J. Kale, G. W. Graham, X. Pan, P. Christopher, *J. Am. Chem. Soc.* **2017**, *139*, 4551–4558.

[3] a) J. Hrbek, F. M. Hoffman, J. B. Park, P. Liu, D. Stacchiola, Y. S. Hoo, S. Ma, A. Nambu, J. A. Rodriguez, M. G. White, *J. Am. Chem. Soc.* **2008**, *130*, 17272–17273; b) T. Uchiyama, H. Yoshida, Y. Kuwauchi, S. Ichikawa, S. Shimada, M. Haruta, S. Takeda, *Angew. Chem. Int. Ed.* **2011**, *50*, 10157–10160; *Angew. Chem.* **2011**, *123*, 10339–10342.

[4] a) G. C. Chinchen, K. C. Waugh, D. A. Whan, *Appl. Catal.* **1986**, *25*, 101–107; b) J. D. Grunwaldt, A. M. Molenbroek, N. Y. Topsøe, H. Topsøe, B. S. Clausen, *J. Catal.* **2000**, *194*, 452–460; c) P. L. Hansen, J. B. Wagner, S. Helveg, J. R. Rostrup-Nielsen, B. S. Clausen, H. Topsøe, *Science* **2002**, *295*, 2053–2055; d) J. Nakamura, Y. Choi, T. Fujitani, *Top. Catal.* **2003**, *22*, 277–285.

[5] a) M. Behrens, F. Studt, I. Kasatkin, S. Kühl, M. Hävecker, F. Abild-Pedersen, S. Zander, F. Girgsdies, P. Kurr, B.-L. Kniep, M. Tovar, R. W. Fischer, J. K. Nørskov, R. Schlögl, *Science* **2012**, *336*, 893–897; b) T. Lunkenbein, J. Schumann, M. Behrens, R. Schlögl, M. G. Willinger, *Angew. Chem. Int. Ed.* **2015**, *54*, 4544–4548; *Angew. Chem.* **2015**, *127*, 4627–4631; c) S. Kuld, M. Thorhauge, H. Falsig, C. F. Elkjær, S. Helveg, I. Chorkendorff, J. Sehested, *Science* **2016**, *352*, 969–974; d) S. Kattel, P. J. Ramírez, J. G. Chen, J. A. Rodriguez, P. Liu, *Science* **2017**, *355*, 1296–1299.

[6] a) C. W. Li, J. Ciston, M. W. Kanan, *Nature* **2014**, *508*, 504–507; b) A. Verdaguer-Casadevall, C. W. Li, T. P. Johansson, S. B. Scott, J. T. McKeown, M. Kumar, I. E. L. Stephens, M. W. Kanan, I. Chorkendorff, *J. Am. Chem. Soc.* **2015**, *137*, 9808–9811; c) A. Eilert, F. Cavalca, F. S. Roberts, J. Osterwalder, C. Liu, M. Favaro, E. J. Crumlin, H. Ogasawara, D. Friebel, L. G. M. Pettersson, A. Nilsson, *J. Phys. Chem. Lett.* **2017**, *8*, 285–290.

[7] T.-J. Huang, D.-H. Tsai, *Catal. Lett.* **2003**, *87*, 173–178.

[8] Z. Zhang, H. Wu, Z. Yu, R. Song, K. Qian, X. Chen, J. Tian, W. Zhang, W. Huang, *Angew. Chem. Int. Ed.* **2019**, *58*, 4276–4280; *Angew. Chem.* **2019**, *131*, 4320–4324.

[9] a) Y. Bu, J. W. H. Niemantsverdriet, H. O. A. Fredriksson, *ACS Catal.* **2016**, *6*, 2867–2876; b) B. Eren, C. Heine, H. Bluhm, G. A. Somorjai, M. Salmeron, *J. Am. Chem. Soc.* **2015**, *137*, 11186–11190.

[10] B. Eren, D. Zherebetskyy, L. L. Patera, C. H. Wu, H. Bluhm, C. Africh, L.-W. Wang, G. A. Somorjai, M. Salmeron, *Science* **2016**, *351*, 475–478.

[11] a) G. Zhou, L. Luo, L. Li, J. Ciston, E. A. Stach, J. C. Yang, *Phys. Rev. Lett.* **2012**, *109*, 235502; b) G. Zhou, L. Luo, L. Li, J. Ciston, E. A. Stach, W. A. Saidi, J. C. Yang, *Chem. Commun.* **2013**, *49*, 10862–10864; c) L. Luo, L. Li, J. Ciston, W. A. Saidi, E. A. Stach, J. C. Yang, G. Zhou, *Phys. Rev. Lett.* **2014**, *113*, 136104.

[12] a) F. Jensen, F. Besenbacher, E. Laegsgaard, I. I. Stensgaard, *Phys. Rev. B* **1990**, *42*, 9206–9209; b) M. Lee, A. J. H. McGaughey, *Surf. Sci.* **2010**, *604*, 1425–1431.

[13] L.-N. Wu, Z.-Y. Tian, W. Qin, *J. Phys. Chem. C* **2018**, *122*, 16733–16740.

Manuscript received: November 25, 2019
Accepted manuscript online: December 9, 2019
Version of record online: December 30, 2019

